Original Research Article

Bio-fabrication and CharacterizationofGreen Synthesized Nanoparticles from Commercial Honey

Abstract

Green approaches to nanoparticle synthesis offer sustainable and environmentally friendly alternatives, avoiding hazardous chemicals typical in traditional methods. This study characterizes nanoparticles synthesized from silver nitrate (AgNO3) and iron oxide (Fe2O3) using commercial honey as a reducing and capping agent.Characterization revealed significant disparities between silver nanoparticles (AgNPs) and iron nanoparticles (FeNPs). AgNPs had a larger particle size (Z-average: 3115.67 nm) compared to FeNPs (Z-average: 1813 nm). AgNPs showed a monodisperse population, while FeNPs had a slightly broader size distribution. Additionally, AgNPs had a higher particle concentration (mean count rate: 505.17 kcps) than FeNPs (mean count rate: 296.65 kcps).Both AgNPs and FeNPs displayed negative surface charges, with AgNPs at -6.499 mV and FeNPs slightly higher at -1.652 mV. Elemental composition analysis by SEM-EDX revealed AgNPs primarily composed of silver, carbon, and oxygen, while FeNPs consisted mainly of iron, oxygen, and carbon.These findings provide insights into the physical and chemical properties of AgNPs and FeNPs synthesized using commercial honey. Understanding these properties is essential for optimizing synthesis processes and exploring applications in medicine, catalysis, and environmental remediation. The eco-friendly synthesis approach using honey underscores the potential for sustainable nanomaterial production. Further research can explore specific applications and benefits of AgNPs and FeNPs synthesized through this green method, offering an efficient and economical alternative for nanoparticle synthesis.

Keywords:nanoparticle synthesis, green approach, commercial honey, characterization, silver nanoparticles, iron nanoparticles

1. Introduction

Over the past two decades, nanotechnology has garnered considerable attention due to its wide-ranging applications across various scientific domains. Among the myriad nanomaterials, metal oxide nanoparticles have emerged as a subject of intensive investigation owing to their distinctive properties (Rostamizadeh et al., 2020). The synthesis of nanomaterials employs diverse methods encompassing physical, chemical, and biological routes (Iravani et al., 2014). Presently, metallic nanoparticles find utility in catalysis, sensor technologies, disease diagnosis, and treatment, among other applications (Galúcio et al., 2022). However, traditional physio-chemical processes for nanoparticle production entail drawbacks such as the generation of harmful chemicals, costly equipment, multistep procedures, and the release of toxic by-products (Mohammadzadeh et al., 2022). Moreover, techniques like lithography, laser ablation, aerosol technologies, and ultraviolet irradiation, though effective, remain financially burdensome. Consequently, there has been a burgeoning interest in employing microorganisms and environmentally benign approaches for nanoparticle synthesis (Nagajyothi et al., 2017). This shift towards simpler, cost-effective, and eco-friendly techniques is increasingly attractive (Jamkhande et al., 2019).

The exploration of plant systems for the biologically assisted synthesis of metal nanoparticles, known as green synthesis, stands as a pivotal endeavor in nanoscience research (Jha et al., 2009). Studies have demonstrated the efficacy of utilizing fungi, algae, bacteria, and plant extracts for the green synthesis of silver nanoparticles (Vijayaraghavan & Nalini, 2010). The development of techniques enabling the controlled synthesis of nanoparticles with precise size, shape, and composition is imperative for their application in diverse fields such as biomedicine, optics, electronics, and water purification (Pradeep, 2009; Allahverdiyev et al., 2011). Recent reports highlight the use of various plant extracts, including coriander leaf, edible mushrooms, algae, cyanobacteria, and fungi, in the biosynthesis of gold and silver nanoparticles. The versatility of nanoparticles, attributed to their diminutive size, typically less than 100 nm, underscores their significance (Shahal, 2020; Gopu et al., 2021). Size reduction confers

distinctive properties upon nanoparticles, such as increased surface area and enhanced magnetic and electrochemical characteristics (Üstün et al., 2022).

Among metallic nanoparticles, silver nanoparticles (Ag-NPs) have garnered significant attention due to their potent antimicrobial activity compared to macroscopic silver (González Fá et al., 2017; Behravan et al., 2019). Natural compounds present in various products, such as alkaloids, phenols, tannins, terpenoids, amino acids, and proteins, facilitate the reduction of Ag+ ions to Ag-NPs, thus stabilizing them and preventing aggregation (Rasheed et al., 2017; Aboyewa et al., 2021; Varadavenkatesan et al., 2016). Silver nanoparticles exhibit exceptional antimicrobial properties, proving effective against a broad spectrum of pathogens including bacteria, fungi, and viruses. Likewise, iron oxide nanoparticles (Fe2O3-NPs), particularly magnetic ones, have gained prominence in applications such as drug delivery, magnetic resonance imaging, and bioremediation (Tufani et al., 2021; Ali et al., 2023). Various chemical methods are employed for the synthesis of Fe2O3-NPs, with recent studies showcasing successful synthesis using aqueous extracts of plants.

Apis mellifera honey, renowned for its therapeutic properties since ancient times, serves as a natural source of nutrition rich in glucose and fructose. Honey-mediated nanoparticle synthesis offers a biocompatible, rapid, and straightforward approach devoid of hazardous by-products, making it suitable for diverse applications (Keskin et al., 2022). Moreover, honey exhibits numerous health benefits, including antimicrobial, antioxidant, anti-inflammatory, and antiviral properties, further accentuating its potential in nanoparticle synthesis and medical applications.

The present study aimed to synthesize and characterize silver and iron nanoparticles (AgNPs, FeNPs) using *Apis mellifera* honey via a green synthesis approach. This endeavor explores the feasibility of utilizing honey as a reducing and capping agent for eco-friendly nanoparticle synthesis at ambient conditions, thereby evaluating their physicochemical properties and potential for various nano-biotechnological applications.

2. Material and Methods

2.1. Biosynthesis of the Nanoparticles, Silver nitrate ($AgNO_3$) and iron oxide (Fe_2O_3) using natural honey

White velvet mesquite organic honey sourced from *Apis mellifera* (honeybee) was procured from the L'Organic online store (Code: LATINHONEY-FIBHJ-17305). In a typical experiment, 20 g of honey was dissolved in 80 ml of deionized water. To prepare a 1 mM solution of silver nitrate ($AgNO_3$), 0.042 g of $AgNO_3$ (Sigma, CAS No: 7761-88-8) was dissolved in 250 ml of deionized distilled water. Subsequently, 20 mL of the prepared 10-3 M $AgNO_3$ solution was added to 15 mL of the honey solution, and the pH was adjusted to 6.5 using 99% pure NaOH (Haiza et al., 2013).

For the green synthesis of iron nanoparticles, a 50% honey solution and 1 mM $FeCl_3.6H_2O$ (Sigma, CAS No: 10025-77-1; 98% pure) were mixed in a 1:1 ratio in a flask. NaOH (99% pure) was then added dropwise to adjust the pH of the solution to 11. Both final solutions were vigorously stirred for 30 minutes on a magnetic stirrer until an intense black colour indicated the formation of Fe_2O_3-NPs, while a golden yellow colour indicated the formation of $AgNO_3$-NPs (Shahid et al., 2023). Centrifugation at 8000 rpm. for 40 minutes was conducted to separate nanoparticles from other particles in the solution. The resulting pellet was washed three times with water and ethanol. An ultra-fine powder of nanoparticles was obtained by drying the solution in a hot air oven at 80°C for 6–7 hours (Bhuiyan et al., 2020).

2.2. Nanoparticle characterization of silver nitrate ($AgNO_3$) and iron oxide (Fe_2O_3)

Nanomaterials synthesized from silver nitrate and iron oxide were characterized using various analytical techniques. The UV-Vis spectrophotometry was initially performed to determine the spectral frequencies of $AgNO_3$-NPs within the range of 200 to 1000 nm and $Fe2O_3$-NPs within the range of 200 to 800 nm. Double-beam UV–Vis spectra were measured using a spectrophotometer (model Victoria, Australia) with two quartz cuvettes, one containing water and the other containing approximately 3 mL of each nanomaterial (Shahid et al., 2023). Pure samples were diluted up to five times to reduce noise, and the experiment was conducted in triplicate for each nanomaterial

from the aqueous honey solution. Subsequently, the UV–visible range was adjusted, and peaks were recorded (Al-Zaban et al., 2019).

The size and zeta potential of the nanoparticles were determined using a Zetasizer system (Malvern Zetasizer ZEN 3600, UK) to assess the distribution size of AgNPs and FeNPs in the colloidal solution. The experiment was conducted in triplicate for each nanomaterial from the aqueous honey solution (Abd El-Aziz and Al-Othman, 2019).

2.3. SEM-EDX Analysis

SEM-EDX Analysis was employed to identify the cellular accumulation of AgNPs and FeNPs, as well as to examine the physical properties including size and shape of honey-treated AgNPs and FeNPs. Samples of honey mediatedAgNPs and FeNPs (25 mL) were centrifuged at 5000 rpm for 10 minutes, washed twice with 0.1X PBS and distilled water, and freeze-dried. The freeze-dried honey suspension was then subjected to SEM-EDX analysis (JSM-6701F, Joel, Japan), which generated distinct X-rays representing the elements present in the sample (Scimeca et al., 2018).

3. Results

3.1. Thebiosynthesis and Spectroscopic Characterization of AgNPs and FeNPs

Apis mellifera honey was recognized as a good source for the synthesis of $AgNO_3$NPs and Fe_2O_3NPs. In the present study, the production of $AgNO_3$NPs and Fe_2O_3NPs started when NaOH was gradually added with stirring to a primary solution containing silver and iron salt combined with sodium hydroxide, the development of a golden yellow color and an intense black color provided a visual indication of the presence of nanoparticles in the solution, respectively.

The synthesis of nanoparticles using aqueous honey solutions (AgNPs-H, FeNPs-H) can be confirmed by measuring the surface plasmon resonance (SPR) band using electronic absorption spectroscopy.The ultraviolet-visible (UV–Vis) spectrum of the reaction mixture has an absorption peak, which showed a sharp peak at 400 nm and350 nm, confirming the surface plasmon resonance of the synthesized $AgNO_3$NPs and Fe_2O_3NPs, respectively.

3.2. Silver and Iron NanoparticlesCharacterization

The results of the particle size measurement (dynamic light scattering method, DLS), zeta potential (laser Doppler electrophoresis method, ZP) of dispersed particles, and the electrolytic conductivity (EC) of the samples showed that the AgNPs synthesis resulted in an increase in the peak height at a particle size of the three replicates of each AgNPs: 3546, 2704, and 3097 nm, with an average of 3116 nm. Meanwhile, the average particle size recorded from FeNPs was 1758, 1868, and 1813, with an average of 1813 nm as shown in Fig. (1). Generally, it is agreed that the particle size and zeta potential of nanoparticles significantly affect their various bioactivities.

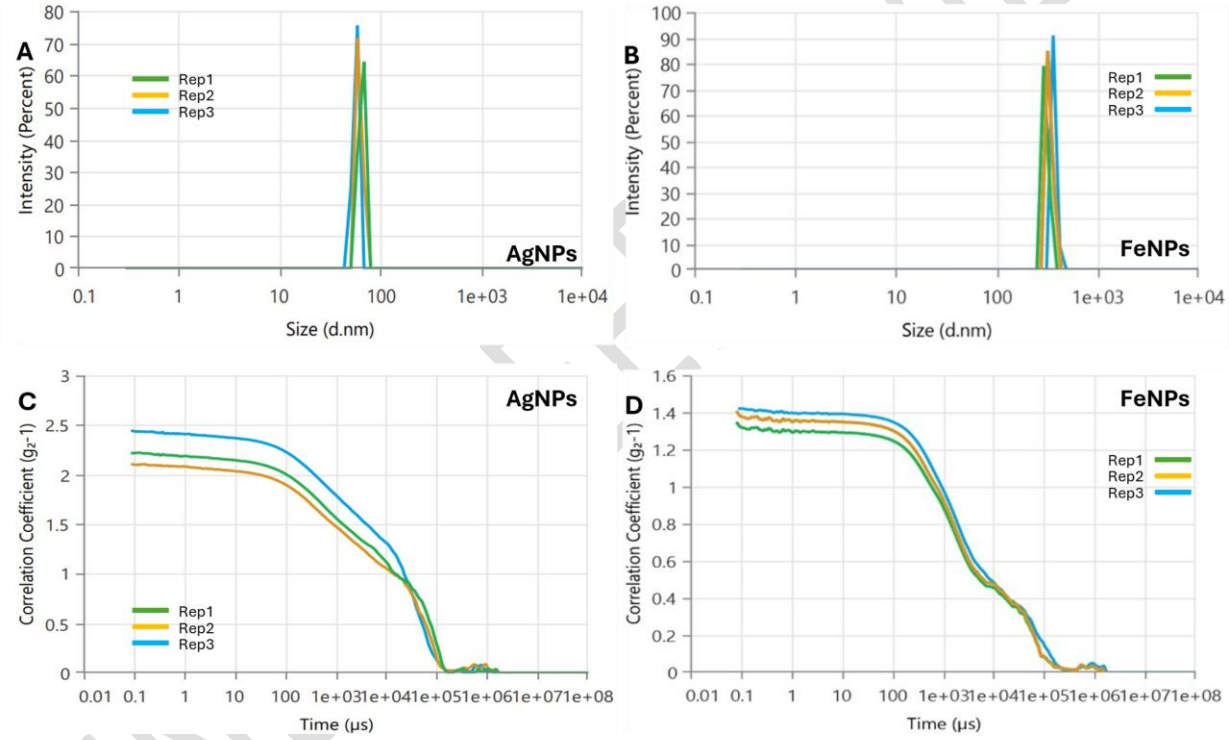

Figure 1. The mean particle size distribution and correlation over time of AgNPs (A, C), and FeNPs (B, D) biosynthesized using commercial honey.

Accordingly, the zeta potential distributions were monomodal for all samples studied. The synthesis of AgNPs showed an increase in the percentage of scattered light intensity observed in the three replicates of AgNPs, which was approximately -6.826, -6487, and -6.184 mV, with an average of -6.499 mV, and a zeta deviation of 2.989 mV, with a conductivity of 0.2066 mS/cm. For FeNPs synthesis, the values were

0.5461, -2.343, and -3.159 mV, with an average of -1.625 mV, and a zeta deviation of 4.663 mV, with a conductivity of 0.08528 mS/cm, as shown in Fig. (2).

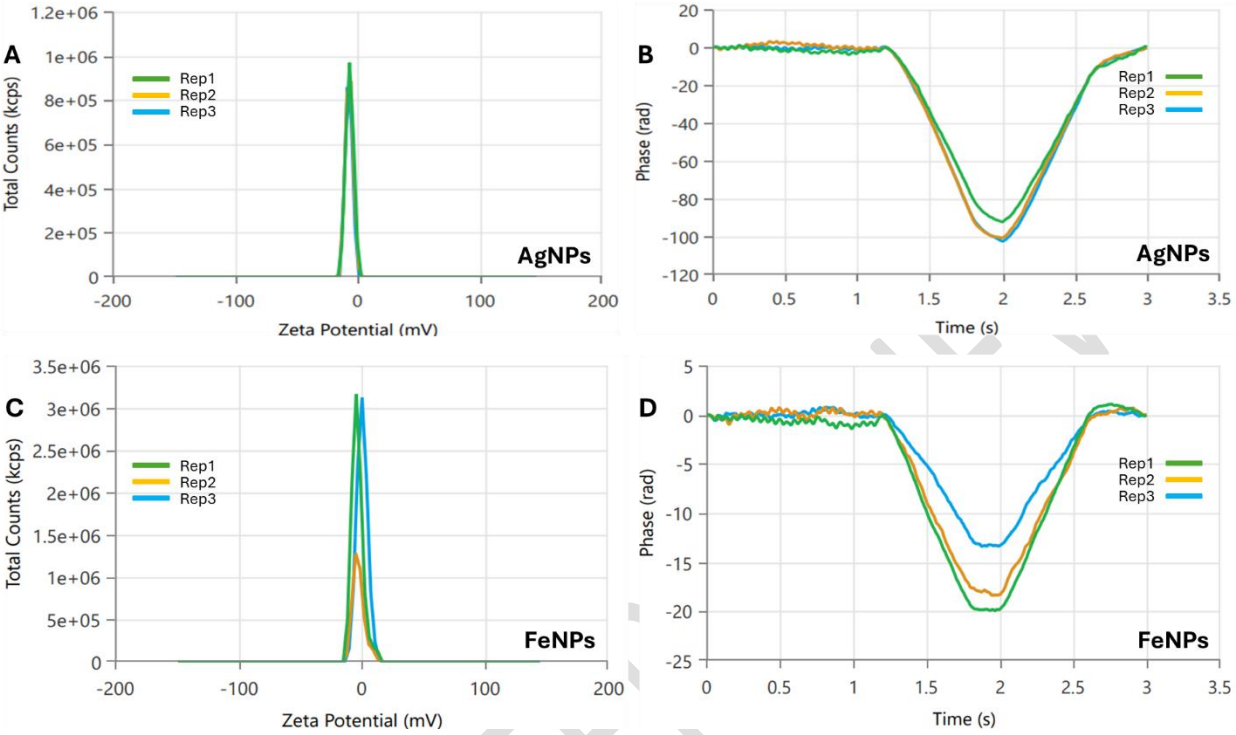

Figure 2. The mean Zeta potential and phase over time of AgNPs (A and B), and FeNPs (C and D) biosynthesized using commercial honey.

3.3 *AgNPs and FeNPs SEM-EDX Analysis*

The Scanning Electron Microscope-Energy Dispersive X-ray (SEM-EDX) was employed to characterize the size, shape, and morphology of AgNPs and FeNPs synthesized at 27°C. An SEM image of AgNPs is shown in Fig#. The images also revealed the presence of a small number of rod-shaped nanoparticles. These structures can form during synthesis, as it is challenging to acquire nanoparticles with consistent specific shapes and sizes. At 19,000x magnification, the average size of AgNPs measured in the images was 42–55 nm.

The reduction of silver (Ag) ions was observed to occur with the addition of NaOH, which acts as a pH regulator. The morphology of silver nanoparticles was obtained from an SEM micrograph. Based on the results, the particle size decreased as the pH of the aqueous solution increased. It can be inferred that there is a rapid

reduction of Ag ions and the formation of smaller nanoparticles at higher pH values. The EDX analysis was employed to examine the elemental composition of the biogenic AgNPs. Oxygen and carbon were the main components revealed by EDX, indicating that the synthesized AgNPs solution contained carbon and oxygen in addition to Ag. This was confirmed by the presence of an α peak between 0.0 and 0.83 keV.

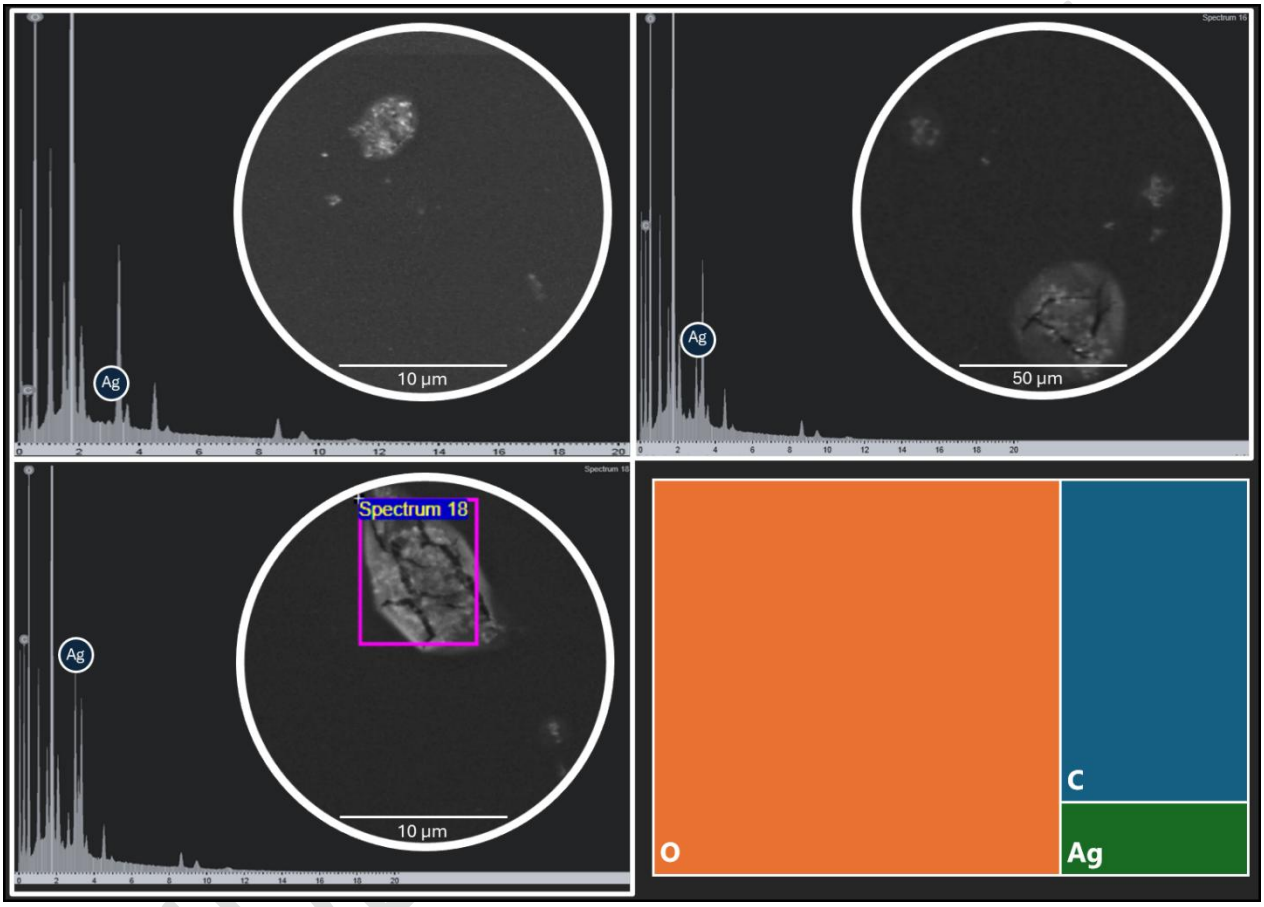

Figure 3. Scanning Electron Microscopy (Sem-EDX) image for Ag nanoparticles synthesized using using commercial honey. The boxplot shows the Weight % for the Carbon (c), Oxygen (O), and Silver (Ag) content collectively from three different scans.

The morphological (size and shape) properties of the produced FeNPs, as determined by SEM, are depicted in Fig.(4). These images confirmed the development of nanostructures, which were well distributed in the solution. A continuous variation was observed in the shape and size of the produced FeNPs. At 19,000x magnification, the size distribution of FeNPs was estimated to be in the range of 100–200 nm with a non-uniform spherical shape. The EDX analysis shown in Figure 2c revealed the

elemental composition of the synthesized FeNPs solution. The α was between 0.0 and 0.83 keV confirmed that Fe and O are present in the synthesized nanoparticles. The abundance of oxygen demonstrated that the nanoparticles are in iron oxide form. Peaks of C and O atoms confirmed the contribution of honey in the synthesis of nanoparticles. The presence of Na and Cl atoms was also detected as impurities in the solution. In the present study, the highest proportion of Fe elements was found in the EDX spectra, indicating that the main component was Fe2O3-NPs.

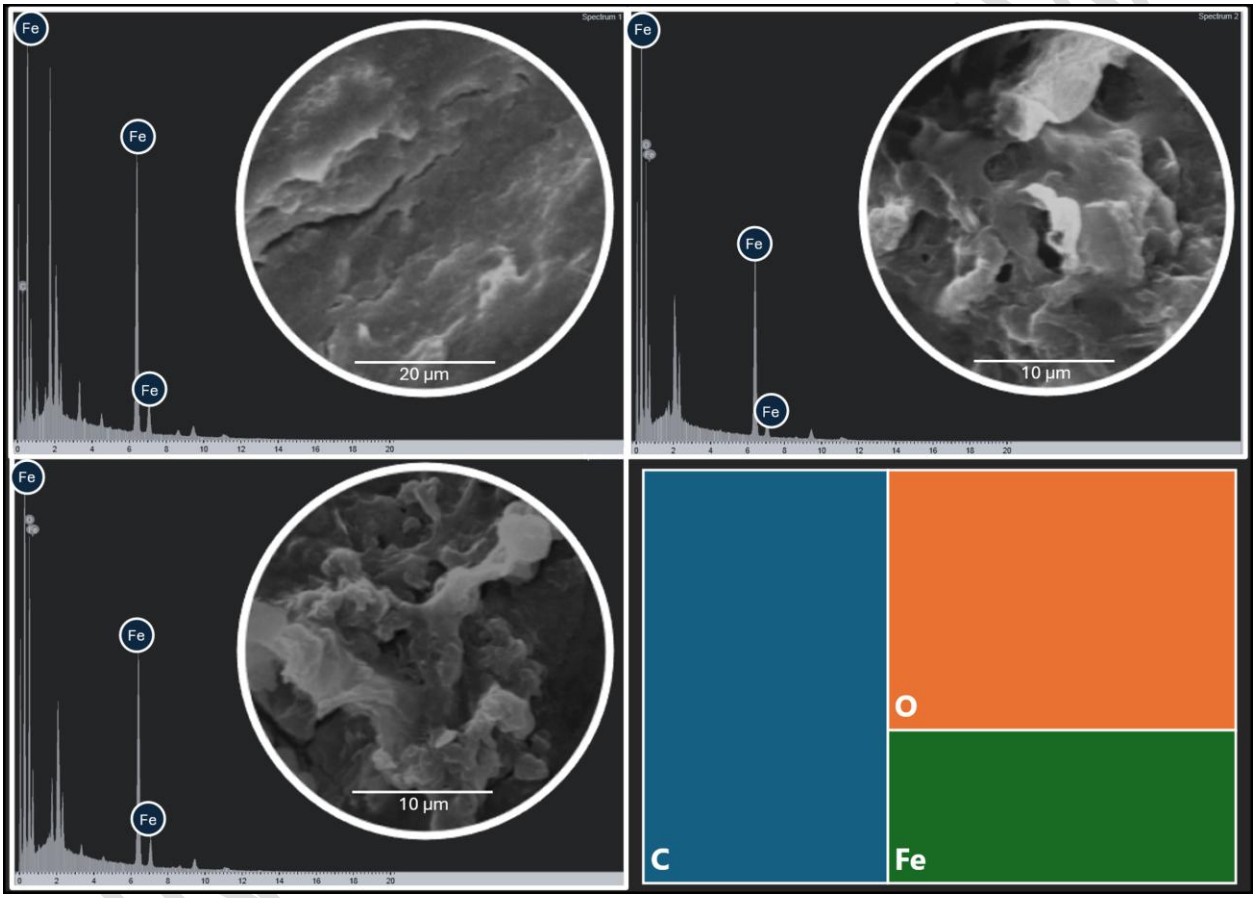

Figure 4. Scanning Electron Microscopy (Sem-EDX) image for Fe nanoparticles synthesized using commercial honey. The boxplot shows the Weight % for the Carbon (c), Oxygen (O), and Iron (Fe) content collectively from three different scans.

3.4Comparative details between AgNO3 and Fe2O3 nanoparticles

The synthesized silver nanoparticles (AgNO3) exhibited a larger Z-average size (3115.67 nm) compared to iron oxide nanoparticles (Fe2O3) (1813 nm), indicating a broader size distribution for AgNO3. However, AgNO3 showed a monodisperse particle

population with a polydispersity index (PI) of 1, while Fe2O3 had a slightly broader size distribution with a PI of 0.9492.In terms of mean count rate, AgNO3 demonstrated a higher value (505.17 kcps) compared to Fe2O3 (296.65 kcps), suggesting a higher particle concentration for AgNO3. The peak 1 mean by intensity ordered by area was smaller for AgNO3 (61.36 nm) than for Fe2O3 (345.35 nm), indicating a smaller primary particle size for AgNO3.Regarding zeta potential, both nanoparticles displayed negative values, with AgNO3 showing a zeta potential of -6.499 mV and Fe2O3 exhibiting a slightly higher negative zeta potential of -1.652 mV. The conductivity values were higher for AgNO3 (0.2066 mS/cm) compared to Fe2O3 (0.08528 mS/cm).Moreover, the wall zeta potential was more negative for AgNO3 (-17.48 mV) than for Fe2O3 (-3.182 mV), indicating a stronger charge at the surface of AgNO3 nanoparticles. However, the zeta deviation was higher for Fe2O3 (4.663 mV) compared to AgNO3 (2.989 mV), suggesting greater variation in zeta potential measurements for Fe2O3.Furthermore, AgNO3 exhibited a significantly higher derived mean count rate (1673 kcps) compared to Fe2O3 (0.00002802 kcps), indicating a higher overall particle count for AgNO3. However, the reference beam count rate values were similar for both nanoparticles, suggesting comparable measurement accuracy.

In addition to the previously mentioned characterization parameters, the SEM-EDX analysis provided insight into the elemental composition of the nanoparticles. For silver nanoparticles (AgNPs), the average weight percentages were determined to be 41.17% for carbon (C), 37.02% for oxygen (O), and 21.80% for iron (Fe). Conversely, iron nanoparticles (FeNPs) exhibited an average weight percentage of 19.89% for carbon (C), 73.11% for oxygen (O), and 7.00% for silver (Ag). These elemental composition percentages highlight the differences in the chemical makeup of the two types of nanoparticles. While both AgNPs and FeNPs contain carbon and oxygen, indicating the presence of organic and oxide components, respectively, the predominant presence of silver in AgNPs and iron in FeNPs distinguishes their elemental compositions.

4. Discussion

Bio-fabrication of metal nanoparticles (NPs) using biological resources as capping and stabilizing agents represents a biocompatible, eco-friendly, and nontoxic approach with widespread biomedical applications. Recently, these nanoparticles have drawn considerable attention owing to the magnetic properties and flexible surface chemistry of iron and silver oxide (Galúcio et al., 2022; Kaur et al., 2021).The outcomes from the present investigation showed that the addition of bee's honey to the silver in the form of nitrate (1 mM) provided a brown color to the mixture that turned from yellow at the start point of addition, indicating the plasmon resonance excitation of AgNPs (Veerasamy et al., 2011), and the addition of iron in the form of an oxide (1 mM) provided an intense black color to the mixture that turned from brown, which provided a visual indication of the presence of nanoparticles in the solution respectively. The mixture color changing in a time-dependent manner was observed, after seven days of keeping in a dark condition, the dark brown color was clear and stable (Shahid et al., 2023).

UV–VIS Spectroscopy was used to observe Ag ions bio-reduction, peaks of 400 and 350 nm were detected for AgNPs, and FeNPs prepared using bee's honey respectively (El-Desouky and Ammar, 2016). During the first stage of the experiment, the synthesis of AgNPs was conducted at a temperature of 25ºC in aqueous honey solutions. A single SPR band indicates that nanoparticles have a spherical shape (Wan et al., 2013).The morphology and surface charge of silver and iron were spherical with average diameters of 3115.67 nm and 1813 nm respectively. The negative zeta potential of biogenic AgNPs was -6.499 mV, and for FeNPs, it was -1.651966667 mV. The surface area of the sorbents changed the morphology of the adsorbent particles and showed agglomeration to large shapes (Kumar et al., 2020).

The negative zeta potential of biogenic AgNPs was recorded at -1.625 mV, consistent with findings from previous studies utilizing honey as a reducing agent (El-Desouky and Ammar, 2016; Mohammed et al., 2018). This negative zeta potential likely contributes to the stability and uniform distribution of AgNPs by inducing particle repulsion (Farhadi et al., 2017). Additionally, negative ionizable groups present in

biomolecules from honey may further contribute to this negative charge, thereby aiding in the dispersion of AgNPs (Khatoon et al., 2017).Conversely, the average zeta potential of iron nanoparticles was measured at -1.625 mV, with a deviation of 4.663 mV. These results suggest that negatively charged groups predominantly constitute the capping biomolecules surrounding the biosynthesized FeNPs (Balasooriya et al., 2017). According to Gengan et al. (2013), a zeta potential exceeding +30 mV or falling below -30 mV indicates a stable system. However, zeta potentials closer to 0 mV are associated with a higher likelihood of particle agglomeration (Guo et al., 2018).

The Scanning electron microscope-energy dispersive X-ray (SEM-EDX) analysis was conducted to determine the cellular accumulation of AgNPs and FeNPs in the aqueous honey solution caused by the treatment of NPs. The SEM images with a magnification of up to 20,000x revealed that the silver and Iron nanoparticle size distribution was in the range of 100 and 200 nm respectively. SEM-ED images showed thatAgNPs reveal spherical shapes and uniform distributions of the nanoparticles, with smooth edges, and without any aggregation observed. The EDX spectrometers have confirmed the presence Ag signal of the AgNPs in the synthesized AgNPs. The percentage of Ag metal found in occurrence with other chemical elements was found to be substantial, about 7%. SEM-EDX was used for element analysis of the biogenic AgNPs prepared in the current study showing the oxygen and carbon as the main components. AgNPs nanostructure prepared from honey and contains carbon and oxygen besides the Ag was also stated by El-Deeb et al. (2015). The other elements originated from honey ingredients such as glucose, fructose, organic acids, vitamins, and minerals and served as capping organic agents bound to the surface of the AgNPs (Femi-Adepoju et al., 2019; Matar et al., 2023). Previous similar research stated AgNPs particles with the same shape and characteristics obtained by bee’s honey collected from different floral sources where SEM and TEM analysis were used (Hosny et al., 2017; El-Deeb et al., 2015). Recent studies have also demonstrated that the size of iron oxide-based nanoparticles is between 10 and 100 nm (Miri et al., 2021; Salama et al., 2022).

In the present study, the shape of FeNPs was estimated to be irregularly spherical. A previous study also reported a cavity-like shape with a rough surface of FeNPs (Ahmad et al., 2021). The SEM images of the present study revealed that the precursor (honey) was stabilizing the surface of nanoparticles by selectively slowing their growth rate and stopping particle aggregation. This result can be correlated with a previous similar study (Sharmila et al., 2022). Another study demonstrated that the nature of FeNPs was not uniform and that they were present mostly in the form of large, agglomerated groups. These clusters were linked to the low capping ability of the plant source and the magnetic properties of FeNPs (Bhuiyan et al., 2020).

The EDX analysis was used to determine the elemental content of the sample. Iron typically exhibits an intense peak at 0.7–7 keV (Biswas et al., 2021). The presence of carbon and oxygen, together with iron, confirmed the involvement of honey in the synthesis of nanoparticle structures. This led to the production of quantitative as well as qualitative evaluations of the iron components that contributed to the generation of FeNPs (Menazea et al., 2020). Cl and Na atoms were also found as residual impurities while synthesizing nanoparticles from ferric chloride, and this has been documented in previous studies (Qasim et al., 2020).

5. Conclusion

A fast, eco-friendly, and convenient green method was used to synthesize AgNPs and FeNPs using honey. By using bees honey, the current study presents detailed results of a bio-reductive green synthesis of silver, and iron nanoparticles (AgNPs, FeNPs). Honey was demonstrated to be a good source of reducing and capping agents to produce stable and well-dispersed AgNPs and FeNPs. Nanoparticles formation was investigated by UV-vis, Zeta potential, and SEM-EDX analysis. The characterization results of silver nanoparticles (AgNPs) and iron nanoparticles (FeNPs) reveal notable distinctions between the two materials. AgNPs exhibit a larger particle size, higher particle concentration, and a more negative zeta potential compared to FeNPs. Additionally, AgNPs display a monodisperse particle population with a broader size distribution, while FeNPs show a slightly broader size distribution. Furthermore, SEM-EDX analysis elucidates the elemental composition of AgNPs and FeNPs, with

AgNPs primarily consisting of silver, carbon, and oxygen, while FeNPs predominantly comprise iron, oxygen, and carbon. These findings underscore the distinct characteristics and compositions of AgNPs and FeNPs, highlighting their potential applications in various fields.

6. References

Abd El-Aziz ARM and Al-Othman MR (2019). Biosynthesized gold nanoparticles using Zingiber officinale and its impact on the growth and chemical composition of lentils (Lens culinaris). *Pak. J. Bot*. 51(2). doi:10.30848/PJB2019-2(21).

Abeska YY and Cavas L (2022). Artificial neural network modelling of green synthesis of silver nanoparticles by honey. *Neural Net.World.* 32(1), 1–14. doi:10.14311/NNW.2022.32.001.

Aboyewa JA, Sibuyi NRS, Meyer M and Oguntibeju OO (2021). Green Synthesis of Metallic Nanoparticles Using Some Selected Medicinal Plants from Southern Africa and Their Biological Applications. *Plants.* 10(9), 1929. doi:10.3390/plants10091929.

Ahmad W, Kumar Jaiswal K and Amjad M (2020).*Euphorbia herita* leaf extract as a reducing agent in a facile green synthesis of iron oxide nanoparticles and antimicrobial activity evaluation. *Inorg. Nano-Metal Chem.*, 1–8. doi:10.1080/24701556.2020.1815062.

Ali I, Pan Y, Jamil Y, Shah AA, Amir M, Al Islam S, Fazal Y, Chen J, and Shen Z(2023). Comparison of copper-based Cu-Ni and Cu-Fe nanoparticles synthesized via laser ablation for magnetic hyperthermia and antibacterial applications. *Physica B: Condens. Matter.* 650, 414503. doi:10.1016/j.physb.2022.414503.

Allahverdiyev AM, Kon KV, Abamor ES, Bagirova M and Rafailovich M (2011). Coping with antibiotic resistance: combining nanoparticles with antibiotics and other antimicrobial agents. *Expert. Rev. Anti. Infect. Ther.* 9(11), 1035–1052. doi:10.1586/eri.11.121.

Al-Othman MR, El-Aziz A, Mohamed AM and Hatamleh AA (2017). Green biosynthesis of silver nanoparticles using pomegranate peel and inhibitory effects of the nanoparticles on aflatoxin production. *Pak. J. Bot.* 49(2), 751–756.

Baimler IV, Lisitsyn AB and Gudkov SV (2020). Water Decomposition Occurring During Laser Breakdown of Aqueous Solutions Containing Individual Gold, Zirconium, Molybdenum, Iron or Nickel Nanoparticles. *Front. Phys.* 8, 620938. doi:10.3389/fphy.2020.620938.

Balasooriya ER, Jayasinghe CD, Jayawardena UA, Ruwanthika RWD, Mendis De Silva R and Udagama PV (2017). Honey Mediated Green Synthesis of Nanoparticles:

New Era of Safe Nanotechnology. *J.Nanomater.* 2017, 1–10. doi:10.1155/2017/5919836.

Behravan M, Hossein Panahi A, Naghizadeh A, Ziaee M, Mahdavi R and Mirzapour A (2019). Facile green synthesis of silver nanoparticles using Berberis vulgaris leaf and root aqueous extract and its antibacterial activity. *Int. J. Biol.Macromol.* 124, 148–154. doi:10.1016/j.ijbiomac.2018.11.101.

Bhuiyan MdSH and others (2020). Green synthesis of iron oxide nanoparticle using Carica papaya leaf extract: application for photocatalytic degradation of remazol yellow RR dye and antibacterial activity. *Heliyon* 6(8), e04603. doi:10.1016/j.heliyon.2020.e04603.

Biswas A, Vanlalveni C, Lalfakzuala R, Nath S and Rokhum SL (2021).*Mikaniamikrantha* leaf extract mediated biogenic synthesis of magnetic iron oxide nanoparticles: Characterization and its antimicrobial activity study. *Mater. Today. Proc.* 42, 1366–1373. doi:10.1016/j.matpr.2021.01.108.

El-Desouky T and Ammar H (2016). Honey mediated silver nanoparticles and their inhibitory effect on aflatoxins and ochratoxin A. *J. App. Pharm. Sci.*, 083–090. doi:10.7324/JAPS.2016.60615.

El-Desouky BS and Mustafa A (2016). New results on higher-order Daehee and Bernoulli numbers and polynomials. *Adv. Differ.Equ.* 2016(1), 32. doi:10.1186/s13662-016-0764-z.

Enbiyale G (2018). Assessment of Honey Production System, Constraints and Opportunities in Ethiopia. *Pharm.Pharmacol. Int. J.* 6(1). doi:10.15406/ppij.2018.06.00153.

Farhadi S, Ajerloo B and Mohammadi A (2017). Green Biosynthesis of Spherical Silver Nanoparticles by Using Date Palm (*Phoenix Dactylifera*) Fruit Extract and Study of Their Antibacterial and Catalytic Activities. *Acta Chim.Slov.*, 129–143.doi:10.17344/acsi.2016.2956.

Femi-Adepoju AG, Dada AO, Otun KO, Adepoju AO and Fatoba OP (2019). Green synthesis of silver nanoparticles using terrestrial fern (*GleicheniaPectinata* (Willd.) C. Presl.): characterization and antimicrobial studies. *Heliyon* 5(4), e01543. doi:10.1016/j.heliyon.2019.e01543.

Galúcio JMP and others (2022). Synthesis, Characterization, Applications, and Toxicity of Green Synthesized Nanoparticles. *Curr. Pharm.Biotechnol.* 23(3), 420–443. doi:10.2174/1389201022666210521102307.

Gengan RM, Anand K, Phulukdaree A and Chuturgoon A (2013). A549 lung cell line activity of biosynthesized silver nanoparticles using *Albizia adianthifolia* leaf. *Colloids Surf. B Biointerfaces.* 105, 87–91. doi:10.1016/j.colsurfb.2012.12.044.

Gericke M and Pinches A (2006). Biological synthesis of metal nanoparticles. *Hydrometallurgy.* 83(1–4), 132–140. doi:10.1016/j.hydromet.2006.03.019.

González Fá AJ, Juan A and Di Nezio MS (2017). Synthesis and Characterization of Silver Nanoparticles Prepared with Honey: The Role of Carbohydrates. *Analytical Letters* 50(5), 877–888. doi:10.1080/00032719.2016.1199558.

Gopu M and others (2021). Green biomimetic silver nanoparticles utilizing the red algae Amphiroa rigida and its potent antibacterial, cytotoxicity and larvicidal efficiency. *Bioprocess.Biosyst. Eng.* 44(2), 217–223. doi:10.1007/s00449-020-02426-1.

Guilger-Casagrande M and Lima RD (2019). Synthesis of Silver Nanoparticles Mediated by Fungi: A Review. *Front.Bioeng.Biotechnol.* 7, 287. doi:10.3389/fbioe.2019.00287.

Guo Y, Zhao Y, Wang S, Jiang C and Zhang J (2018). Relationship between the zeta potential and the chemical agglomeration efficiency of fine particles in flue gas during coal combustion. *Fuel.* 215, 756–765. doi:10.1016/j.fuel.2017.11.005.

Haiza H, Azizan A, Mohidin AH and Halin DSC (2013). Green Synthesis of Silver Nanoparticles Using Local Honey. *Nano Hyb.* 4, 87–98. doi:10.4028/www.scientific.net/NH.4.87.

Hassanisaadi M, Bonjar AHS, Rahdar A, Varma RS, Ajalli N and Pandey S (2022). Eco-friendly biosynthesis of silver nanoparticles using Aloysia citrodora leaf extract and evaluations of their bioactivities. *Mater. Today Commun.* 33, 104183. doi:10.1016/j.mtcomm.2022.104183.

Hosny AMS, Kashef MT, Rasmy SA, Aboul-Magd DS and El-Bazza ZE (2017). Antimicrobial activity of silver nanoparticles synthesized using honey and gamma radiation against silver-resistant bacteria from wounds and burns. *Adv. Nat. Sci.: Nanosci.Nanotechnol.* 8(4), 045009. doi:10.1088/2043-6254/aa8b44.

Hossain ML, Lim LY, Hammer K, Hettiarachchi D and Locher C (2022). A Review of Commonly Used Methodologies for Assessing the Antibacterial Activity of Honey and Honey Products. *Antibiotics.* 11(7), 975. doi:10.3390/antibiotics11070975.

Jamkhande PG, Ghule NW, Bamer AH and Kalaskar MG (2019). Metal nanoparticles synthesis: An overview on methods of preparation, advantages and disadvantages, and applications. *J. Drug. Deliv. Sci. Technol.* 53, 101174. doi:10.1016/j.jddst.2019.101174.

Jha AK, Prasad K, Prasad K and Kulkarni AR (2009). Plant system: Nature's nanofactory. *Colloids Surf. B Biointerfaces.* 73(2), 219–223. doi:10.1016/j.colsurfb.2009.05.018.

Kasthuri J, Veerapandian S and Rajendiran N (2009). Biological synthesis of silver and gold nanoparticles using apiin as reducing agent. *Colloids Surf. B Biointerfaces.* 68(1), 55–60. doi:10.1016/j.colsurfb.2008.09.021.

Keskin M, Kaya G and Keskin S (2022). Nanotechnology in Honey: Future and Perspectives Honey as Nanoparticles. Bhattacharya T and Ahmed S eds. *Nanotechnol. Func. Foods*. Wiley, 87–101. doi:10.1002/9781119905059.ch4.

Khatoon N, Mazumder JA and Sardar M (2017).Biotechnological Applications of Green Synthesized Silver Nanoparticles. *J.Nanosci. Curr. Res.* 02(01). doi:10.4172/2572-0813.1000107.

Kumar AS, Madhu G, John E, Kuttinarayanan SV and Nair SK (2020). Optical and antimicrobial properties of silver nanoparticles synthesized via green route using honey. *Green Proces.Synt.* 9(1), 268–274. doi:10.1515/gps-2020-0029.

Lozhkomoev AS and others (2021). Synthesis of Fe/Fe3O4 core-shell nanoparticles by electrical explosion of the iron wire in an oxygen-containing atmosphere. *J.Nanopart. Res.* 23(3), 73. doi:10.1007/s11051-021-05180-x.

Mandey F, Ainunnisa, Zakir M and Noor A (2019). Utilization of polyfloral honey in the synthesis of gold nanoparticles and evaluation of its potency as an antibacterial against S. aureus and E. coli. *J. Phys.: Conf. Ser.* 1341(3), 032007. doi:10.1088/1742-6596/1341/3/032007.

Matar GH, Akyüz G, Kaymazlar E and Andac M (2022). An Investigation of Green Synthesis of Silver Nanoparticles Using Turkish Honey Against Pathogenic Bacterial Strains. *Biointerface Res Appl Chem* 13(2), 195. doi:10.33263/BRIAC132.195.

Menazea AA and Ahmed MK (2020). Silver and copper oxide nanoparticles-decorated graphene oxide via pulsed laser ablation technique: Preparation, characterization, and photoactivated antibacterial activity. *Nano-Struct. Nano-Obj.* 22, 100464. doi:10.1016/j.nanoso.2020.100464.

Miri A, Najafzadeh H, Darroudi M, Miri MJ, Kouhbanani MAJ and Sarani M (2021). Iron Oxide Nanoparticles: Biosynthesis, Magnetic Behavior, Cytotoxic Effect. *ChemistryOpen.* 10(3), 327–333. doi:10.1002/open.202000186.

Mohammadzadeh V and others (2022). Applications of plant-based nanoparticles in nanomedicine: A review. *Sustain. Chem. Pharm.* 25, 100606. doi:10.1016/j.scp.2022.100606.

Mohammed A, Al-Qahtani A, al-Mutairi A, Al-Shamri B and Aabed K (2018). Antibacterial and Cytotoxic Potential of Biosynthesized Silver Nanoparticles by Some Plant Extracts. *Nanomater.* 8(6), 382. doi:10.3390/nano8060382.

Mora-Godínez S, Abril-Martínez F and Pacheco A (2022). Green synthesis of silver nanoparticles using microalgae acclimated to high CO2. *Mater. Today: Proc.* 48, 5–9. doi:10.1016/j.matpr.2020.04.761.

Nagajyothi PC, Pandurangan M, Kim DH, Sreekanth TVM and Shim J (2017). Green Synthesis of Iron Oxide Nanoparticles and Their Catalytic and In Vitro Anticancer Activities. *J.Clust. Sci.* 28(1), 245–257. doi:10.1007/s10876-016-1082-z.

Patel V, Berthold D, Puranik P and Gantar M (2015). Screening of cyanobacteria and microalgae for their ability to synthesize silver nanoparticles with antibacterial activity. *Biotechnol. Rep.* 5, 112–119. doi:10.1016/j.btre.2014.12.001.

Patil KR, Jung K and Eickhoff SB (2023) Commentary on Pang et al. (2023).*Nat. Neurosci*. Preprint. doi:10.1101/2023.10.06.561240.

Patil SP, Chaudhari RY and Nemade MS (2022).Azadirachta indica leaves mediated green synthesis of metal oxide nanoparticles: A review. *Talanta Open.* 5, 100083. doi:10.1016/j.talo.2022.100083.

Philip D (2009). Biosynthesis of Au, Ag and Au–Ag nanoparticles using edible mushroom extract. *Spectrochim. Acta A.* 73(2), 374–381. doi:10.1016/j.saa.2009.02.037.

Pradeep T and Anshup (2009). Noble metal nanoparticles for water purification: A critical review. *Thin Solid Films.* 517(24), 6441–6478. doi:10.1016/j.tsf.2009.03.195.

Priya, Naveen, Kaur K and Sidhu AK (2021). Green Synthesis: An Eco-friendly Route for the Synthesis of Iron Oxide Nanoparticles. *Front.Nanotechnol.* 3, 655062. doi:10.3389/fnano.2021.655062.

Qasim S and others (2020). Green synthesis of iron oxide nanorods using Withaniacoagulans extract improved photocatalytic degradation and antimicrobial activity. *J. Photochem. Photobiol.* 204, 111784. doi:10.1016/j.jphotobiol.2020.111784.

Rasheed T, Bilal M, Iqbal HMN and Li C (2017). Green biosynthesis of silver nanoparticles using leaves extract of Artemisia vulgaris and their potential biomedical applications. *Colloids Surf. B Biointerfaces*. 158, 408–415. doi:10.1016/j.colsurfb.2017.07.020.

Rizvi M, Bhatia T and Gupta R (2022). Green & sustainable synthetic route of obtaining iron oxide nanoparticles using *Hylocereus undantus* (pitaya or dragon fruit). *Mater. Today: Proc.* 50, 1100–1106. doi:10.1016/j.matpr.2021.07.469.

Rodney S and Purdy J (2020). Dietary requirements of individual nectar foragers, and colony-level pollen and nectar consumption: a review to support pesticide exposure assessment for honey bees. *Apidologie.* 51(2), 163–179. doi:10.1007/s13592-019-00694-9.

Rostamizadeh E, Iranbakhsh A, Majd A, Arbabian S and Mehregan I (2020). Green synthesis of Fe2O3 nanoparticles using fruit extract of *Cornus mas* L. and its growth-promoting roles in Barley. *J.Nanostruct. Chem.* 10(2), 125–130. doi:10.1007/s40097-020-00335-z.

Salama AM, Abedin RMA and Elwakeel KZ (2022). Influences of greenly synthesized iron oxide nanoparticles on the bioremediation of dairy effluent using selected microbial isolates. *Int. J. Environ. Sci. Technol.* 19(8), 7019–7030. doi:10.1007/s13762-021-03625-3.

Scimeca M, Bischetti S, Lamsira HK, Bonfiglio R and Bonanno E (2018). Energy Dispersive X-ray (EDX) microanalysis: A powerful tool in biomedical research and diagnosis. *Eur. J.Histochem*. 62(1). doi:10.4081/ejh.2018.2841.

Shah AA and others (2020). Facile synthesis of copper doped ZnO nanorods for the efficient photo degradation of methylene blue and methyl orange. *Ceram. Int.* 46(8), 9997–10005. doi:10.1016/j.ceramint.2019.12.024.

Shahid H and others (2023). Synthesis, Characterization, and Biological Properties of Iron Oxide Nanoparticles Synthesized from Apis mellifera Honey. *Molecules*. 28(18), 6504. doi:10.3390/molecules28186504.

Sharmila M and others (2022). Photocatalytic Dye Degradation and Bio-Insights of Honey-Produced α-Fe2O3 Nanoparticles. *Water.* 14(15), 2301. doi:10.3390/w14152301.

Stolyar SV and others (2021). Polysaccharide-coated iron oxide nanoparticles: Synthesis, properties, surface modification. *Mater. Lett.* 284, 128920. doi:10.1016/j.matlet.2020.128920.

Tufani A, Qureshi A and Niazi JH (2021). Iron oxide nanoparticles based magnetic luminescent quantum dots (MQDs) synthesis and biomedical/biological applications: A review. *Mater. Sci. Eng. C.* 118, 111545. doi:10.1016/j.msec.2020.111545.

Üstün E, Önbaş SC, Çelik SK, Ayvaz MÇ and Şahin N (2021). Green Synthesis of Iron Oxide Nanoparticles by Using Ficus Carica Leaf Extract and Its Antioxidant Activity. *Biointerface. Res. Appl. Chem.* 12(2), 2108–2116. doi:10.33263/BRIAC122.21082116.

Van Den Berg AJJ, Van Den Worm E, Quarles Van Ufford HC, Halkes SBA, Hoekstra MJ and Beukelman CJ (2008). An *in vitro* examination of the antioxidant and anti-inflammatory properties of buckwheat honey. *J. Wound. Care.* 17(4), 172–178. doi:10.12968/jowc.2008.17.4.28839.

Varadavenkatesan T, Selvaraj R and Vinayagam R (2016). Phyto-synthesis of silver nanoparticles from Mussaendaerythrophylla leaf extract and their application in

catalytic degradation of methyl orange dye. *J. Mol. Liq.* 221, 1063–1070. doi:10.1016/j.molliq.2016.06.064.

Veerasamy R and others (2011). Biosynthesis of silver nanoparticles using mangosteen leaf extract and evaluation of their antimicrobial activities. *J. Saudi Chem. Soc.* 15(2), 113–120. doi:10.1016/j.jscs.2010.06.004.

Velgosova O, Mražíková A, Čižmárová E and Málek J (2018). Green synthesis of Ag nanoparticles: Effect of algae life cycle on Ag nanoparticle production and long-term stability. *Trans. Nonferrous Met. Soc. China.* 28(5), 974–979. doi:10.1016/S1003-6326(18)64732-6.

Vijayaraghavan R, Chandrashekar R, Jyothiprakash AM and Belagavi CS (2010). Isolated tuberculous osteomyelitis of the scapula. *Case Rep.* bcr0420102889–bcr0420102889. doi:10.1136/bcr.04.2010.2889.

Vijayaraghavan K and Nalini SPK (2010).Biotemplates in the green synthesis of silver nanoparticles. *Biotechnol. J.* 5(10), 1098–1110. doi:10.1002/biot.201000167.

Wan Y and others (2013). Quasi-spherical silver nanoparticles: Aqueous synthesis and size control by the seed-mediated Lee–Meisel method. *J. Colloid. Interface Sci.* 394, 263–268. doi:10.1016/j.jcis.2012.12.037.